Al_2O_3 on WSe_2 by Ozone Based Atomic Layer Deposition: Nucleation and Interface Study

UT Dallas Author(s):

Angelica Azcatl
Qingxiao Wang
Moon J. Kim
Robert M. Wallace

Citation:

Azcatl, Angelica, Qingxiao Wang, Moon J. Kim, and Robert M. Wallace. 2017. "Al_2O_3 on WSe_2 by ozone based atomic layer deposition: Nucleation and interface study." APL Materials 5(8), doi:10.1063/1.4992120

Al_2O_3 on WSe_2 by ozone based atomic layer deposition: Nucleation and interface study

Angelica Azcatl, Qingxiao Wang, Moon J. Kim, and Robert M. Wallace

Citation: APL Materials **5**, 086108 (2017); doi: 10.1063/1.4992120
View online: https://doi.org/10.1063/1.4992120
View Table of Contents: http://aip.scitation.org/toc/apm/5/8
Published by the American Institute of Physics

APL MATERIALS **5**, 086108 (2017)

Al_2O_3 on WSe_2 by ozone based atomic layer deposition: Nucleation and interface study

Angelica Azcatl, Qingxiao Wang, Moon J. Kim, and Robert M. Wallace[a]
Department of Materials Science and Engineering, The University of Texas at Dallas, 800 West Campbell Road, Richardson, Texas 75080, USA

(Received 26 June 2017; accepted 9 August 2017; published online 22 August 2017)

In this work, the atomic layer deposition process using ozone and trimethylaluminum (TMA) for the deposition of Al_2O_3 films on WSe_2 was investigated. It was found that the ozone-based atomic layer deposition enhanced the nucleation of Al_2O_3 in comparison to the water/TMA process. In addition, the chemistry at the Al_2O_3/WSe_2 interface and the surface morphology of the Al_2O_3 films exhibited a dependence on the deposition temperature. A non-covalent functionalizing effect of ozone on WSe_2 at low deposition temperatures 30 °C was identified which prevented the formation of pinholes in the Al_2O_3 films. These findings aim to provide an approach to obtain high-quality gate dielectrics on WSe_2 for two-dimensional transistor applications. [http://dx.doi.org/10.1063/1.4992120]

Monolayer WSe_2 is a promising channel material for 2D electronic device applications, demonstrating a hole-mobility in the order of 250 cm^2/V s when implemented in field-effect transistors.[1] Furthermore, it has been proposed that the formation of a $WSe_2/SnSe_2$ heterostructure can lead to a nearly broken band alignment, which is a desirable property for an efficient interband tunneling for thin-tunneling field-effect transistor applications.[2] Recently, several efforts towards the growth or deposition of WSe_2 films have been reported.[3,4] However, the envisioned device applications for WSe_2 such as top-gate FETs or tunneling FETs also requires the integration of dielectric films on the WSe_2 surface. In this regard, the dearth of dangling bonds at the WSe_2 surface has shown to prevent the uniform deposition of films by atomic layer deposition (ALD).[5] Previously, Park *et al.*[6] proposed the use of a seed layer based on titanylphthalocyanine (TiOPc) molecules deposited by molecular beam epitaxy (MBE) on WSe_2 in order to generate nucleation sites for the subsequent ALD process. While this technique achieved uniform Al_2O_3 deposition on the $TiOPc/WSe_2$ structure, the process required an additional MBE step prior ALD. In this work, we propose an alternative approach to deposit Al_2O_3 on WSe_2 which consists in the use of ozone as oxidant precursor during the ALD process. Ozone-based ALD has been proven to generate thin Al_2O_3 films on graphene[7] and MoS_2.[8] Here, the conditions during the ozone-based ALD process are critical as ozone can cause oxidation[9] or etching[3] of WSe_2. In this work, the nucleation and reactivity upon deposition of Al_2O_3 on WSe_2 using ozone and TMA was investigated by *in situ* X-ray photoelectron spectroscopy characterization (XPS). The deposition temperature was identified as a critical parameter for the resulting interfacial chemistry for Al_2O_3 on WSe_2. Based on the temperature dependence study, an ozone-based ALD process is proposed where oxidation of WSe_2 is avoided while a uniform and pinhole free Al_2O_3 dielectric film is obtained.

For these experiments, synthetic bulk WSe_2 (2D Semiconductors, Inc.) was employed. The initial surface was prepared by mechanical exfoliation of the outermost layers using Scotch® Magic™ tape. The freshly exfoliated surface was immediately loaded (within 5 min) into an ultrahigh vacuum (UHV) system. Then, the WSe_2 sample was annealed at 300 °C for 2 h under UHV (~10^{-9} mbar) to remove the adsorbed carbon from the surface due to the short air exposure after exfoliation.

[a]Author to whom correspondence should be addressed: rmwallace@utdallas.edu

After annealing, the adsorbed carbon signal in the C 1*s* XPS spectrum was below the detection limit. The annealed WSe_2 surface was then transferred *in situ* to the ALD chamber to perform the Al_2O_3 deposition by the ozone-based ALD, where TMA was the metal-organic precursor and ozone the oxidant precursor. TMA was introduced into the reactor with a pulse time of 0.1 s, followed by a 4 s Ar purge. Ozone was generated from a remote source (TMEIC OP-250H-LT generator at an ozone concentration of ~380 g/Nm^3), using a pulse time of 0.1 s and a flow of ~70 SCCM followed by a purge time of 10 s to complete one cycle. In order to analyze the interface chemistry between the Al_2O_3 film and WSe_2 by XPS, all the depositions were performed using 30 ALD cycles at different temperatures. The *in situ* XPS characterization was performed in an ultrahigh vacuum (UHV) system described elsewhere[10] using an Al Kα source (hν = 1486.7 eV) and an Omicron EA125 hemispherical 7-channel analyzer. The XPS scans were acquired at a takeoff angle of 45° with respect to the sample normal and pass energy of 15 eV. For XPS peak analysis and deconvolution, the software *AAnalyzer* was employed, setting Voigt line shapes and an active Shirley background for peak fitting.[11] AFM characterization was performed using an atomic probe microscope, Veeco, Model 3100 Dimension V, on tapping mode under air ambient conditions. The processing of the AFM images was performed using WSXM 4.0 software.[12] A cross section specimen has been prepared using a focused ion beam (FIB, FEI Nano 200) for the Al_2O_3/WSe_2 interface study. Scanning transmission electron microscopy-annular bright field (STEM-ABF) imaging was performed using a Cs-corrected JEM-ARM200F operated at 200 kV.

First, the effect of the deposition temperature on the film uniformity and surface roughness of Al_2O_3 deposited on WSe_2 was investigated. For this study, atomic force microscopy imaging was carried out on the Al_2O_3 films deposited at a temperatures range of 30 °C–300 °C using 30 cycles of TMA and O_3 for all the depositions. For comparative purposes, Al_2O_3 was also deposited on WSe_2 by the conventional water-based ALD approach using 30 cycles of TMA and H_2O at the same range of temperatures studied for the TMA/ozone case (see supplementary material). Figure 1 shows the variation in surface morphology for Al_2O_3 deposited at different temperatures on WSe_2. Interestingly, the 30 °C deposition temperature shows low surface roughness and complete coverage. The uniform nucleation for Al_2O_3 at low ALD temperatures is analogous to the behavior reported previously for graphene[7,13,14] and MoS_2,[8] suggesting a possible non-covalent ozone interaction with WSe_2. For the same temperature, the dielectric nucleation for the H_2O based ALD process was non-uniform. As the temperature increased to 100 °C, Al_2O_3 islands were obtained (height ~ 2-4 nm), indicating that the effectiveness of the nucleation degraded in comparison to the deposition at 30 °C. The uniform deposition at 30 °C is indicative of a uniform ozone physisorption on the WSe_2 surface, whereas the island growth obtained at 100 °C suggests partial desorption of the weakly absorbed ozone promoted by an increase in thermal energy. In addition, as described previously for MoS_2, island growth results from the combination of limited number of reactive sites at the surface and weak adsorption of the ALD precursors at the nucleation stage.[15] For the depositions performed at 150 °C, 200 °C, and 300 °C, the Al_2O_3 island growth was avoided, however pinholes were still present in the films as shown in the height line scan in Fig. 1.

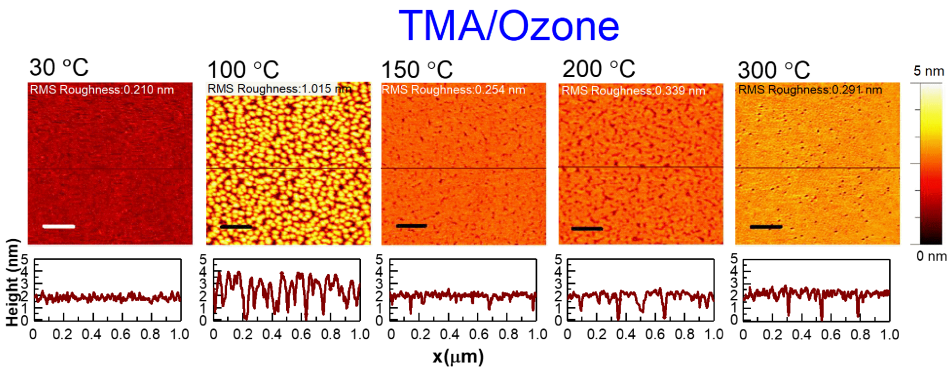

FIG. 1. AFM images and height profiles of ALD-Al_2O_3 films deposited using TMA and ozone on WSe_2 at various temperatures. Scale bar: 200 nm.

To further understand the ozone-based ALD Al_2O_3 nucleation on WSe_2, the interface chemistry was investigated by *in situ* XPS. Figure 2(a) shows the XPS spectra for WSe_2 (Se 3d and W 4f) after Al_2O_3 using 30 cycles of TMA/ozone at different temperatures. There was neither evidence of chemical bonding between WSe_2 and Al_2O_3 at deposition temperatures of 30 °C, 100 °C, and 150 °C nor oxidation of WSe_2, indicating that the chemical integrity of WSe_2 was preserved and that the interaction between these materials is non-covalent. Increasing the deposition temperature to 200 °C caused the formation of substoichiometric WO_x ($x < 3$) detected at a binding energy of ~36.0 eV. In addition to WO_x, WSe_x peaks were detected at 0.5 eV lower in binding energy than the bulk WSe_2 peaks for W 4*f* and Se 3*d*, which is indicative of partial (non-uniform) etching of the outermost WSe_2 layers. The fact that no selenium oxide species were detected is consistent with desorption of such species from the surface during the oxidative etching process. This situation highlights the reactivity of WSe_2 towards oxidation, whereas in the case of MoS_2, the TMA/O_3 process did not cause oxidation at 200 °C as reported by Park *et al.*[6]

In order to determine whether ozone itself could have oxidized WSe_2, ozone exposure was performed on WSe_2 at 200 °C. Figure S3 of the supplementary material shows that after 30 pulses of ozone, the exposure leads to formation of WSe_x and a low intensity peak in O 1s develops, this can be regarded as an initial stage of the oxidation process. By extending the ozone exposure using 60 pulses, WO_x is detected on the surface which indicates that only after a long ozone exposure the oxidation in WSe_2 can occur at 200 °C. Therefore, the WSe_2 oxidation obtained after Al_2O_3 deposition is likely promoted not only by ozone but also by additional reactive species, such as atomic oxygen, generated during the reaction between TMA and ozone.[16]

The Al_2O_3 deposition at 300 °C resulted in oxidation of WSe_2, forming WO_3 (~36.2 eV) and a higher oxidation state at a binding energy of ~36.7 eV, corresponding to a tungstate compound according to the literature.[17] Given the tendency of WO_3 to react with Al_2O_3 to form $Al_2(WO_4)_3$, such a compound is most likely present at the interface and is correlated to the peak at 36.7 eV.[18] It was also found that, in contrast to the deposition at 200 °C, no WSe_x peaks in either W 3*d* or Se 3*d* spectra were detected at 300 °C, suggesting a uniform oxidation of the WSe_2 outermost surface.

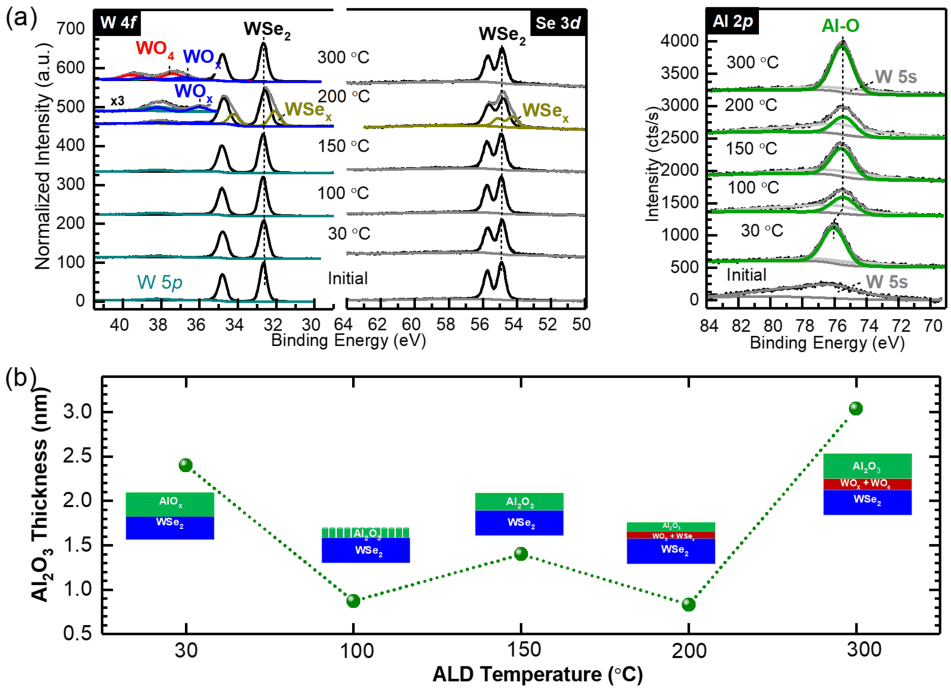

FIG. 2. (a) XPS spectra (W 4*f*, Se 3*d*, and Al 2*p* core levels) of the Al_2O_3/WSe_2 interface upon ALD using 30 cycles of TMA/ozone at different temperatures. (b) Al_2O_3 thickness vs ALD deposition temperature estimated from the XPS spectra shown in Fig. 1.

Based on the chemical analysis, it can be stated that in order to avoid the presence of an interfacial oxide layer using ozone-based ALD on WSe_2, the deposition should be performed at or below 150 °C. The corresponding Al 2*p* spectra before and after Al_2O_3 deposition for all the studied temperatures are presented in Fig. 2(a). Here it should be noted that the W 5*s* peak spans the Al 2*p* region, and careful peak fitting was required to subtract the contribution of such peak to the Al–O integrated intensity. The Al 2*p* spectra show a single chemical state for the Al–O bond after deposition using the ozone-based ALD process. Interestingly, the Al–O peak for the deposition performed at 30 °C is detected at higher in binding energy (~0.6 eV) than the Al–O peaks obtained at higher temperatures. This binding energy shift can be related to the effect of Al–OH bonds present in the Al_2O_3 film due to incomplete removal of –OH groups at low temperatures; this increase in binding energy for the Al–O peak is consistent with previous reports for Al_2O_3 deposited by ozone-based ALD on Si at low temperatures.[19]

In order to determine the effect of the deposition temperature with the Al_2O_3 growth rate, the Al_2O_3 thickness was estimated from the signal attenuation of W 4*f* due to the overlayer film (obtained after 30 ALD cycles) with respect to the initial W 4*f* peak from bulk WSe_2. The estimated thickness also accounted for the oxide interlayer (IL) thickness, if present, following the procedure described by Vitchev *et al.* for a multilayer stack.[20] Figure 2(c) shows the Al_2O_3 growth rate trend, which is closely related to the surface morphology and interface chemistry. For example, the Al_2O_3 thickness obtained at 100 °C decreased in comparison to 30 °C due to the island growth mode non-uniform nucleation. Another drop in thickness was identified at 200 °C which can be related to the formation of WO_x and partial etching of WSe_2 during the ALD process. The deposition at 300 °C led to a significant increase in Al_2O_3 thickness, even when an oxide IL was formed. This suggests that at 300 °C, the reaction towards the formation of Al_2O_3 is favorable even when there were parallel reactions to form WO_3 and $Al_2(WO_4)_3$.

To further improve the nucleation of Al_2O_3 on WSe_2 and to avoid the presence of pinholes in the films, the use of an Al_2O_3 seed layer deposited by ozone-based ALD at low temperature was investigated. According to the results from the temperature dependence study, the deposition at 30 °C leads to uniform and complete film coverage on WSe_2 without the presence of an oxide IL. Also, taking into account that –OH groups will be developed at 30 °C, only a thin seed layer is employed to promote the nucleation of Al_2O_3, and a second deposition is then performed at higher temperature also by ozone-based ALD. In this study, the seed layer consisted of 15 cycles of TMA/O_3 at 30 °C, followed by the Al_2O_3 deposition at 200 °C using 30 cycles of TMA/O_3. *In situ* XPS was performed at each stage and the measured spectra are presented in Fig. 3. It was found that upon

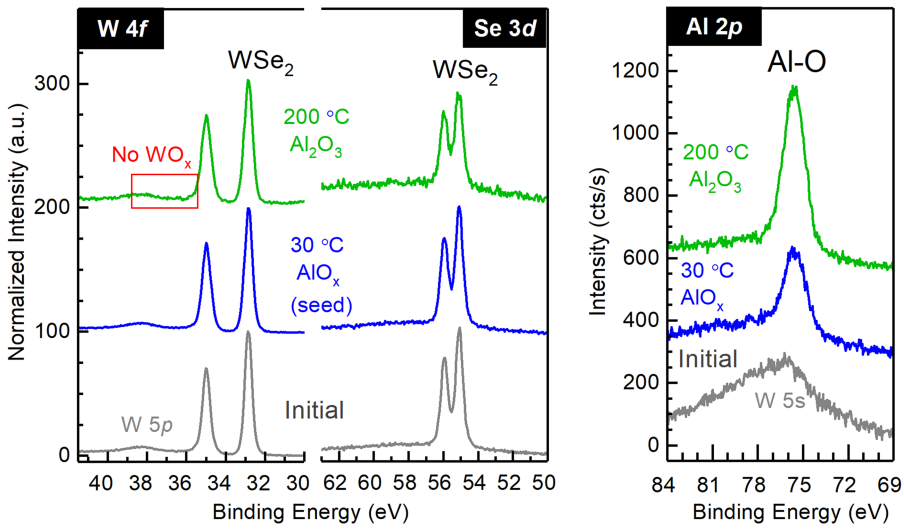

FIG. 3. W 4*f*, Se 3*d*, and Al 2*p* XPS core levels of WSe_2 before and after deposition of a low-temperature AlO_x seed layer, followed by the deposition of Al_2O_3 at 200 °C.

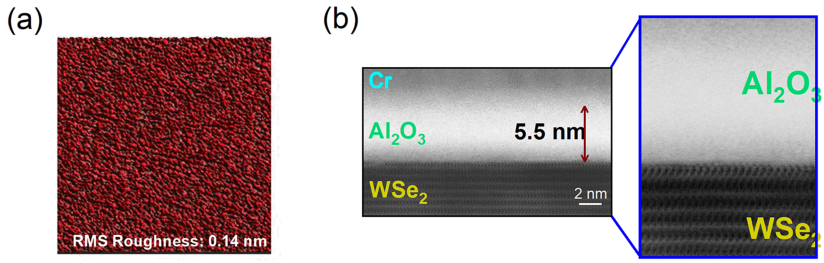

FIG. 4. (a) Surface morphology by AFM and (b) cross-sectional STEM-ABF image of the film obtained after the 2-step ozone-based ALD deposition (low-temperature seed layer AlO_x + Al_2O_3 at 200 °C) on WSe_2.

deposition of the low-temperature seed layer, no changes in the chemical state of WSe_2 occurred. This is consistent with the lack of reactivity observed for ozone only with WSe_2 as presented in Fig. 2(a). In addition, the Al 2*p* spectra show a single peak for the Al–O bond at 75.6 eV and an O/Al ratio of 1.6:1. The estimated thickness of the 15-cycles AlO_x seed layer from the signal attenuation of W 4*f* is ~0.7 nm. After a subsequent Al_2O_3 deposition at 200 °C, no evidence of interfacial oxidation or WSe_x species was detected by XPS. Therefore, the presence of the seed layer prior the higher temperature ALD process prevented the partial etching and oxidation of WSe_2. In fact, the presence of a low-temperature seed layer enhanced the ALD nucleation of the film grown at 200 °C since the resulting surface morphology of the film shows high uniformity, decreasing the root-mean-square roughness up to 0.14 nm. Furthermore, the Al_2O_3 film was pinhole-free, which was confirmed by cross-sectional STEM imaging shown in Fig. 4. Also, a clean and sharp interface was obtained by the ozone-based ALD process described here, with a total thickness of 5.5 nm for the Al_2O_3 film.

In conclusion, an ozone-based ALD process was evaluated for the deposition of thin Al_2O_3 on WSe_2. It was found that the interfacial chemistry, deposition rate, and surface topography of Al_2O_3 exhibited a significant dependence on the deposition temperature. This study provides a temperature window for the optimal deposition of Al_2O_3 by ozone-based ALD on WSe_2, which can serve to prevent oxidation and etching of WSe_2. Finally, the use of a uniform low-temperature AlO_x seed layer was found to enhance the nucleation for the Al_2O_3 films grown at a conventional ALD temperature (200 °C) and also prevented the oxidation of the underlying WSe_2 substrate. This work provides a fundamental understanding of the ozone based-ALD technique to obtain thin and uniform Al_2O_3 films on WSe_2. The electrical performance of the Al_2O_3 is under evaluation, with possible interest and application in device structures such as 2D top-gated FETs and TFETs.

See supplementary material, which is available on-line, for the description of AFM measurements of the WSe_2 surface morphology obtained after 30 ALD cycles of TMA/H_2O at various temperatures, as well as XPS spectra of Al_2O_3 deposited by ozone-based ALD on WSe_2 and the effect of the ozone exposure on WSe_2 at 200 °C.

This work is supported in part by the Center for Low Energy Systems Technology (LEAST), one of six centers supported by the STARnet phase of the Focus Center Research Program (FCRP), a Semiconductor Research Corporation program sponsored by MARCO and DARPA.

[1] H. Fang, S. Chuang, T. C. Chang, K. Takei, T. Takahashi, and A. Javey, Nano Lett. **12**, 3788 (2012).
[2] M. O. Li, D. Esseni, J. J. Nahas, D. Jena, and H. G. Xing, IEEE J. Electron Devices Soc. **3**, 200 (2015).
[3] S. M. Eichfeld, L. Hossain, Y. Lin, A. F. Piasecki, B. Kupp, A. G. Birdwell, R. A. Burke, N. Lu, X. Peng, J. Li, A. Azcatl, S. McDonnell, R. M. Wallace, M. J. Kim, T. S. Mayer, J. M. Redwing, and J. A. Robinson, ACS Nano **9**, 2080 (2015).
[4] J. K. Huang, J. Pu, C. L. Hsu, M. H. Chiu, Z. Y. Juang, Y. H. Chang, W. H. Chang, Y. Iwasa, T. Takenobu, and L. J. Li, ACS Nano **8**, 923 (2014).
[5] A. Azcatl, S. KC, X. Peng, N. Lu, S. McDonnell, X. Qin, F. de Dios, R. Addou, J. Kim, M. J. Kim, K. Cho, and R. M. Wallace, 2D Mater. **2**, 014004 (2015).
[6] J. H. Park, S. Fathipour, I. Kwak, K. Sardashti, C. F. Ahles, S. F. Wolf, M. Edmonds, S. Vishwanath, H. G. Xing, S. K. Fullerton-Shirey, A. Seabaugh, and A. C. Kummel, ACS Nano **10**, 6888 (2016).
[7] S. Jandhyala, G. Mordi, B. Lee, G. Lee, C. Floresca, P.-R. Cha, J. Ahn, R. M. Wallace, Y. J. Chabal, M. J. Kim, L. Colombo, K. Cho, and J. Kim, ACS Nano **6**, 2722 (2012).
[8] L. Cheng, X. Qin, A. T. Lucero, A. Azcatl, J. Huang, R. M. Wallace, K. Cho, and J. Kim, ACS Appl. Mater. Interfaces **6**, 11834 (2014).

[9] M. Yamamoto, S. Dutta, S. Aikawa, S. Nakaharai, K. Wakabayashi, M. S. Fuhrer, K. Ueno, and K. Tsukagoshi, Nano Lett. **15**, 2067 (2015).
[10] R. M. Wallace, in *ECS Transactions* (ECS, 2008), pp. 255–271.
[11] A. Herrera-Gómez, A. Hegedus, and P. L. Meissner, Appl. Phys. Lett. **81**, 1014 (2002).
[12] I. Horcas, R. Fernández, J. M. Gómez-Rodríguez, J. Colchero, J. Gómez-Herrero, and A. M. Baro, Rev. Sci. Instrum. **78**, 013705 (2007).
[13] B. Lee, S. Y. Park, H. C. Kim, K. Cho, E. M. Vogel, M. J. Kim, R. M. Wallace, and J. Kim, Appl. Phys. Lett. **92**, 203102 (2008).
[14] S. McDonnell, A. Pirkle, J. Kim, L. Colombo, and R. M. Wallace, J. Appl. Phys. **112**(10), 104110 (2012).
[15] S. McDonnell, B. Brennan, A. Azcatl, N. Lu, H. Dong, C. Buie, J. Kim, C. L. Hinkle, M. J. Kim, and R. M. Wallace, ACS Nano **7**, 10354 (2013).
[16] S. D. Elliott, G. Scarel, C. Wiemer, M. Fanciulli, and G. Pavia, Chem. Mater. **18**, 3764 (2006).
[17] W. Grüner, E. S. Shpiro, R. Feldhaus, K. Anders, G. V. Antoshin, and Kh. M. Minachev, J. Catal. **107**, 522 (1987).
[18] L. Salvati, L. E. Makovsky, J. M. Stencel, F. R. Brown, and D. M. Hercules, J. Phys. Chem. **85**, 3700 (1981).
[19] S. K. Kim, S. W. Lee, C. S. Hwang, Y.-S. Min, J. Y. Won, and J. Jeong, J. Electrochem. Soc. **153**, F69 (2006).
[20] R. G. Vitchev, J. J. Pireaux, T. Conard, H. Bender, J. Wolstenholme, and C. Defranoux, Appl. Surf. Sci. **235**, 21 (2004).

Supplementary Material

Al_2O_3 on WSe_2 by Ozone based Atomic Layer Deposition: Nucleation and Interface Study

Angelica Azcatl[1], Qingxiao Wang[1], Moon J. Kim[1] and Robert M. Wallace[1]*

[1]Department of Materials Science and Engineering, The University of Texas at Dallas, 800 West Campbell Road, Richardson, Texas 75080, United States

1. Water-based ALD for Al_2O_3 deposition on WSe_2

The WSe_2 surface is characterized by the inertness of the basal plane.[1,2] This situation represent a limitation for a conventional atomic layer deposition process on bare WSe_2. For example, the deposition of Al_2O_3 using trimethyl-aluminum and water by ALD results in non-uniform nucleation and formation of alumina clusters or islands. Here, the presence of sporadic defects at the atomic scale potentially served as nucleation sites during the ALD process. The bright regions in Figure S1 correspond to Al_2O_3 clusters, whereas the dark areas represent the bare WSe_2 surface. The height line profile shows that the density and height of the Al_2O_3 clusters varied with deposition temperature. Here, the nucleation is limited for all the temperatures by the dearth of reactive sites (dangling bonds) at the WSe_2 surface. The deposition temperatures of 200 °C and 300 °C exhibited a very low density of Al_2O_3 clusters, which is possibly dominated by precursor desorption, whereas at 100 °C, incomplete reactivity of the precursors could be the cause of the limited nucleation of Al_2O_3 on WSe_2. In contrast, the ozone-based ALD approach was proven to enhance the ALD nucleation for the same number of cycles. This situation can be related to the limited interaction between H_2O and the WSe_2 surface in the ALD process, in agreement with the studies by Mayer, et al.[3] where it was found that water does not react with WSe_2; instead, a weak water absorption was observed only at low temperatures (140 K), whereas complete water desorption is expected to occur at room temperature under UHV.

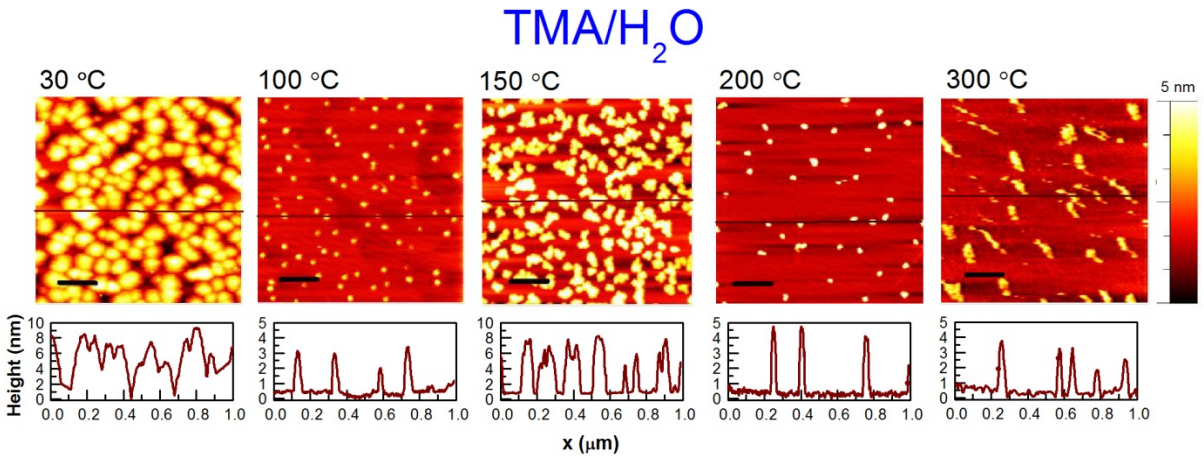

Figure S1. AFM surface morphology obtained after 30 ALD cycles of TMA/H_2O on WSe_2 at various temperatures. Scale bar: 200 nm.

2. C 1*s* and O 1*s* XPS spectra of Al_2O_3 deposited by Ozone-based ALD on WSe_2

The C 1*s* and O 1*s* XPS spectra provide important information for the analysis of the ozone-based ALD process on WSe_2. First, the as-exfoliated WSe_2 surface shows an initial single peak in the C 1s region that corresponds to adventitious carbon, developed on the WSe_2 surface due to the air exposure after mechanical exfoliation. In addition, the peaks at binding energies of 285.7 eV and 296.9 eV correspond to selenium Auger features which overlap with carbon related peaks. After peak fitting, such features were deconvoluted for the accurate identification of the C 1*s* signals. Upon deposition by ALD at 30 °C using 30 cycles of TMA/ozone, a clear carbonate signal was detected at binding energy of ~291. eV. The carbonate specie is a by-product from the TMA/ozone combustion-like reaction, in agreement with previous reports.[4,5] A low-intensity C-H peak was also detected related to an incomplete reaction of the methyl groups from TMA. The intensity of the carbonate peak decreased by increasing the deposition temperature, and at 300 °C, such peak was below the detection limit. In correlation with these results, the O 1*s* spectra show the contribution of the carbonate and –OH groups to the signal in addition to the expected Al-O peak from Al_2O_3. At deposition temperatures of 200 °C and 300 °C, additional features corresponding to W-O bonds were identified at 533.0 eV. It is also worth noting that the presence of hydroxyl groups was significantly reduced at 200 °C and 300 °C, which can be beneficial to the dielectric properties of Al_2O_3.

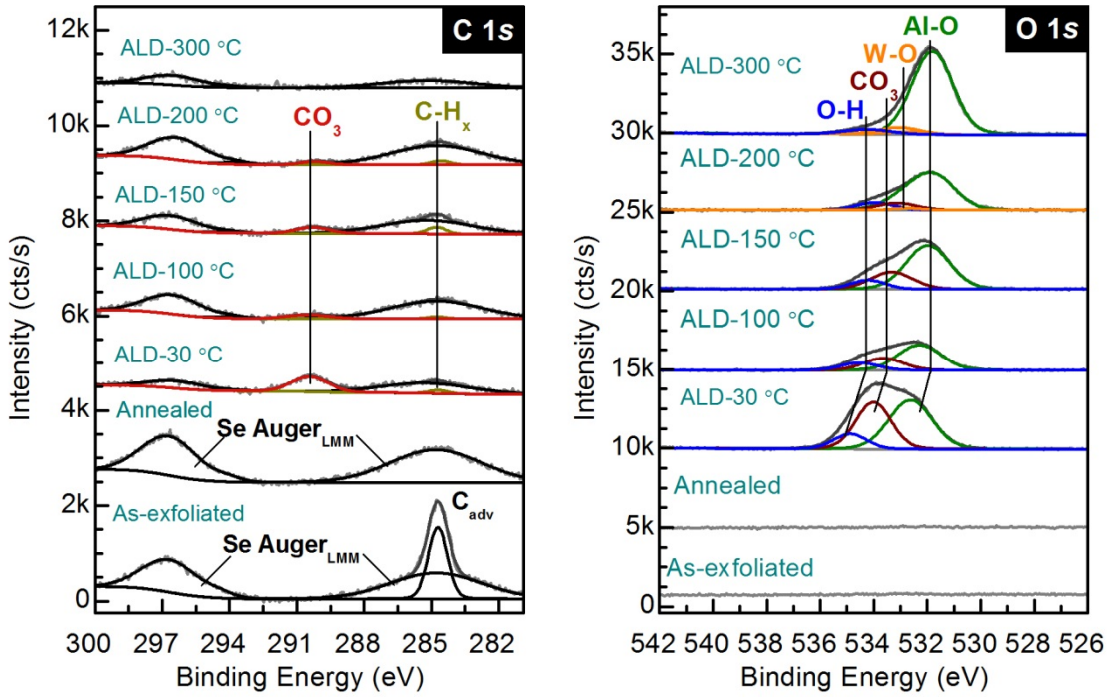

Figure S2. C 1*s* and O 1*s* XPS core levels of WSe_2 before and after deposition of Al_2O_3 by ozone-based ALD at various temperatures.

3. Ozone exposure on WSe_2 at 200 °C

In this study, it was found that a WO_x interlayer was formed after Al_2O_3 deposition at 200 °C. To further understand the oxidation of WSe_2 upon ozone-based ALD processing, the ozone exposure on WSe_2 was studied. The ozone exposures were performed in the same ALD chamber and conditions employed for the ALD Al_2O_3 studies but without TMA pulsing. As shown in Figure S3, after the ozone exposure using 30 cycles, not evident oxidation of WSe_2 was detected by XPS, i.e. WO_x or SeO_x were below the detection limit. However, the ozone exposure did generate a low-intensity signal in the O 1*s* region along with WSe_x features that can be interpreted as an initial stage of the surface oxidation due to the partial replacement of Se with O in WSe_2. The surface morphology of the ozone exposure surface shows the formation of cluster-like features that resemble those observed in oxidized MoS_2 by oxygen plasma exposure.[6] The extended ozone exposure (60 cycles) leads to oxidation of WSe_2, forming WO_3 at the surface. The fact that the oxidized surface is uniform and smooth indicates that a complete oxidation of WSe_2 basal plane was achieved, consistent with the absence of WSe_x peaks. As mentioned previously, ozone by itself can cause oxidation of WSe_2 but only after long exposures at this temperature, whereas the ALD process using TMA/ozone the oxidation readily occurred after 30 ALD cycles.

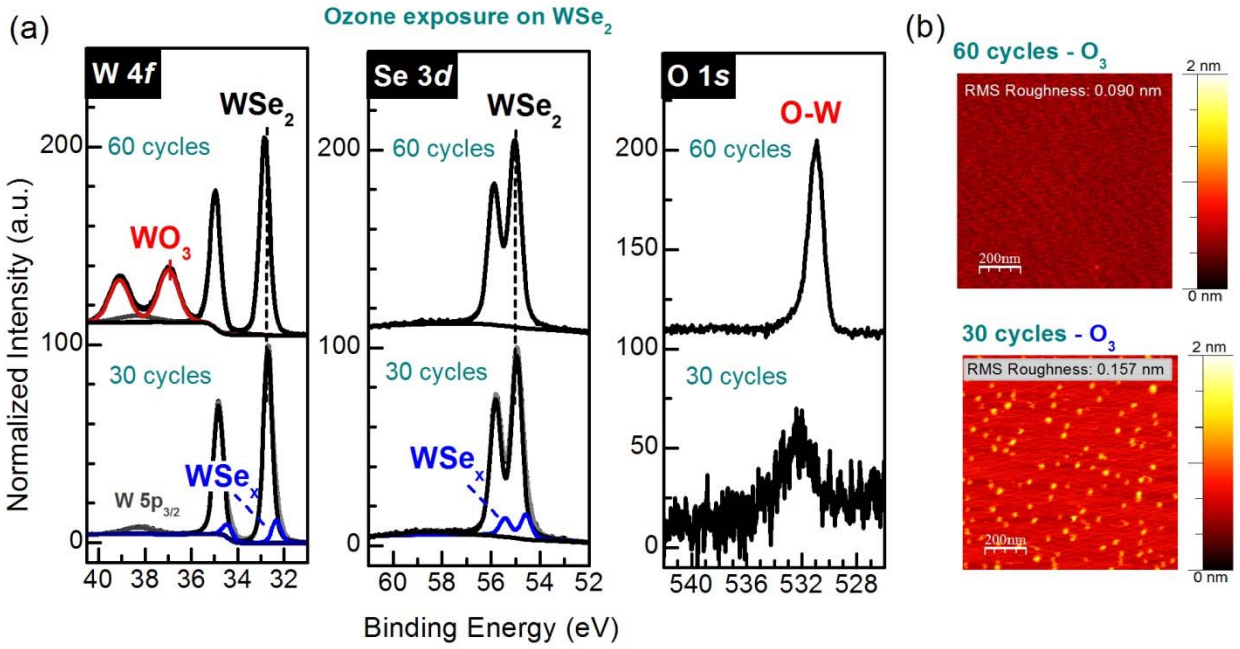

Figure S3. (a) XPS spectra of WSe_2 and (b) surface morphology by AFM after 30 cycles and 60 cycles of ozone exposures on WSe_2 at 200 °C.

References

[1] R. Addou and R.M. Wallace, ACS Appl. Mater. Interfaces **8**, 26400 (2016).
[2] C. Tsai, K. Chan, F. Abild-Pedersen, and J.K. Nørskov, Phys. Chem. Chem. Phys. **16**, 13156 (2014).
[3] T. Mayer, A. Klein, O. Lang, C. Pettenkofer, and W. Jaegermann, Surf. Sci. 269–270, 909 (1992).
[4] V.R. Rai, V. Vandalon, and S. Agarwal, Langmuir **28**, 350 (2012).
[5] J. Kwon, M. Dai, M.D. Halls, and Y.J. Chabal, Chem. Mater. **20**, 3248 (2008).
[6] H. Zhu, X. Qin, L. Cheng, A. Azcatl, J. Kim, and R.M. Wallace, ACS Appl. Mater. Interfaces **8**, 19119 (2016).

RSC Adv., 2017, 7, 884 (2017)